Published in final edited form as:
J Phys Chem A. 2006 May 4; 110(17): 5901–5908. doi:10.1021/jp0573588.

Equilibrium geometries and associated energetic properties of mixed metal- silicon clusters from global optimization

Jianhua Wu and **Frank Hagelberg**
Computational Center for Molecular Structure and Interactions, Department of Physics, Atmospheric Sciences, and General Science, Jackson State University, Jackson, MS 39217, USA

Abstract

The structural properties of the cluster series Me_mSi_{7-m} (Me=Cu and Li, $m \leq 6$) are studied by density functional theory (DFT) employing a plane wave basis. The equilibrium geometries and energetic properties of these clusters are obtained by use of the simulated annealing procedure in conjunction with the Nosé thermostat algorithm. The lowest energy isomer thus obtained is analyzed by Density Functional Theory at the B3LYP/6−311+G(d,p) level including all electrons. Pentagonal ground state structures derived from the D_{5h} equilibrium geometries of both Si_7 and Cu_7 are obtained for Cu_mSi_{7-m} with $m < 6$. The Li_mSi_{7-m} clusters, in contrast, tend towards adsorption geometries where m Li atoms are attached to a Si_{7-m} framework with pronounced negative charge. For both Li_mSi_{7-m} and Cu_mSi_{7-m}, a marked decrease of the energy gap is found as the number of metal atom constituents increases. 61.46.+w, 73.22.-f, 36.40.Qv, 36.40.Cg

Introduction

Atomic Clusters containing no more than a few hundred particles have been shown to display pronounced size-dependent properties,[1] such as geometric and electronic structure, binding energy, melting temperature. A large and rapidly growing range of applications has been identified for nanoclusters. Thus, in view of their very favorable surface/volume ratio, these species have been utilized as catalysts.[2] More recently, much attention has been paid to the use of nanoclusters in a biological context. For example, gold nanoparticles studded with short segments of DNA[3] could form the basis of an easy-to-read procedure for identifying genetic sequences[4].

Substantial efforts of both theorists and experimentalists have focused on elucidating the geometric, electronic and energetic features of pure silicon clusters.[5-15] These studies were motivated chiefly by the fundamental interest in the size evolution of silicon from the scale of several atoms to the crystalline phase as well as the prospect of applications in the field of electronic materials. Photodissociation[5] and collision-induced dissociation experiments have shown that both Si_6 and Si_{10} have exceptional stability, consistent with their “magic” behavior as observed in the mass spectra of Si clusters.[6]

The electronic structure of small metal clusters has long been a subject of intensive theoretical and experimental studies, because of its importance for the understanding of metal-metal interactions and its relevance for catalysis and photography. Alkali metal clusters, such as sodium and lithium clusters,[16-20] have received most attention, which is related to the simplicity of these systems, with each metal atom contributing only one valence electron. Further, detailed investigations have been devoted to transition-metal clusters, and among them prominently noble metal clusters.[21-23]

At low temperatures, the most favored structure of a cluster of *N* particles is the one that minimizes its total energy. Within the Born-Oppenheimer approximation the preferred

geometry is given by the global minimum of the total cluster energy as a function of the coordinates of the atomic cores, defining the potential-energy surface (PES). In the case of Li clusters (Li_N), systematic *ab initio* configuration-interaction studies for N≤9 have shown that the lowest isomers are planar up to the pentamer.[18] At N=6, Ishikawa *et al.*[19] reported a three-dimension D_{4h} structure with slightly lower energy than the planar triangle and the pentagonal pyramid.

The energetics of small copper clusters has been extensively treated in a recent review by Alonso.[21] Several *ab initio* calculations[21] have been performed for N≤10, again comparing a set of plausible structures. There is evidence of planar equilibrium shapes up to N=5 or N=6 maximum, as suggested by recent density functional theory (DFT) calculations.[22] For N=13, DFT computations indicate a preference of the icosahedron over the cuboctahedron.[23]

The structures of Si_n (n=4−13) clusters have been studied extensively by both *ab initio* and density functional approaches. For a review, the reader is referred to ref.[11]. The ground state of Si_4 is a planar rhombus (D_{2h}) in the neutral and anionic states. The ground state of Si_5 is a compressed trigonal bipyramid (D_{3h}) while Si_6 and Si_7 adopt the structures of a C_{2v} edge-capped trigonal bipyramid and a D_{5h} pentagonal-bipyramid, respectively. The latter geometry has also been identified as the equilibrium structure of the metal clusters Li_7[18] and Cu_7[22].

Metal-doped silicon clusters exhibit a richer variety of geometric arrangements than pure silicon clusters. The metal atom in the Si_n cluster stabilizes the pure Si cluster. Beck[24] used a laser vaporization supersonic expansion technique to investigate $MeSi_n$ (Me=Cu, Cr, Mo, and W) clusters by means of mass-spectrometry and reported that they turned out to be more stable towards photofragmentation than bare Si_n clusters of similar size. Employing an ion trap method, Hiura *et al.*[25] produced metal atom encapsulating Si cluster ions of composition $MeSi_n^+$ (Me=Hf, Ta, W, Re, Ir, etc., with n=9,11,12,13,14). Further analysis revealed that Si_n cluster with endohedral metal atom impurities are characterized by enhanced stability, strong size selectively, and a large energy gap between the highest occupied molecular orbital (HOMO) and the lowest unoccupied molecular orbital (LUMO). The respective experimental findings stimulated several computational projects on the geometric, electronic and energetic properties of metal-doped silicon clusters.[12, 26-30]

Mixed species combined of both types of constituents, metal and semiconductor components, have been shown to occur at the metal-semiconductor interface.[31,32] These hybrids are of substantial impact on the properties of the interface as well as the semiconductor. Clusters of the form Cu_xSi_y, containing multiple copper atoms, were detected in experiment.[31,32] To our knowledge, no theoretical investigation on these species has been presented so far. In this contribution we study the geometric and energetic features of Me_mSi_{7-m} (Me=Cu and Li, m ≤ 6) clusters. The choice of these systems is motivated by the similarity of the pure Si_7, Li_7, and Cu_7 clusters which all stabilize in D_{5h} symmetry, thus imposing 'symmetry boundary conditions' on Me_mSi_{7-m} (Me = Cu and Li, m=1,2,...,6). On the other hand, Li and Cu, representing the alkali group (IA) and the noble metal group (IB) of the periodic system, are expected to display strongly differing behavior when integrated into a Si_n cluster. Thus, the most loosely bound electron of Li is easily transferred to the Si constituents. In Li_mSi_n clusters, therefore, Li atoms will act as electron donors, and Si atoms as the receptors. Cu atoms, however, have been shown to form covalent bonds with Si atoms[12,33], and, correspondingly, to adopt substitutional positions in Si_n clusters.[34] How does this fundamental difference impact the geometries, stabilities and bonding features of the mixed species Me_mSi_{7-m} with Me = Li, Cu?

To eliminate the dependence on the initial geometry, and to reduce the probability for trapping the system in a higher than the lowest minimum of the potential energy surface, a global

optimization scheme has to be applied as opposed to a local relaxation method. The need for a global procedure is strongly intensified in the present case where species consisting of mixed constituents are considered since the set of candidate structures is increased by the number of possible permutations of the two differing elements. The simulated annealing approach[7] has been demonstrated to be successful in identifying global minima, although it met with some difficulties for large clusters.

In this work, we employ *ab initio* molecular dynamics on the basis of the simulated annealing method[35,36] to investigate species of the form Me_mSi_{7-m} (Me=Cu and Li, $m \leq 6$) clusters. In order to confirm the lowest energy isomers we have also applied various quantum chemical methods including density functional theory (DFT) at the B3LYP/6−311+G(d,p) level taking all electrons into account.

In the following, we outline the computational method; subsequently, the calculated results are presented and discussed. Finally, we add some concluding remarks.

Theoretical approach

Global geometry optimizations have been performed using the Density Functional Theory (DFT) based Vienna *ab initio* Simulation Package (VASP).[35,36] More specifically, the finite temperature version of Local Density Functional (LDF) Theory, as developed by Mermin,[37] is utilized in conjunction with the exchange-correlation functional given by Ceperley and Alder and parameterized by Perdew and Zunger.[38] It has been shown that the Hellmann-Feynman scheme yields a valid description of the forces within the DFT formalism also at finite temperature. Instead of Fermi-Dirac broadening of the one-electron energies, it may be computationally convenient to choose Gaussian broadening which is used in this contribution. The width of the Gaussian distribution was selected as 0.01eV, the total energy of the system refers to the limit of vanishing width.

The generalized Kohn-Sham equations[39] are solved employing a residual minimization scheme, namely the direct inversion in the iterative subspace (RMM-DIIS) method.[40,41] The interaction between valence electrons and core ions is described by the projector-augmented wave (PAW) method[42] applying a generalized gradient correction (GGA), where the exchange correlation functional of Perdew and Wang[43] (PW91) was used. In the case of Li atoms, all electrons (1s and 2s shell) are treated as valence electrons; the energy cut-off for plane wave basis set is chosen as E_{cut}=272 eV, while that for the augmentation charges is E_{aug}=428 eV. For Cu atoms, 3d and 4s electrons are included in the valence system; the values for the energy cut-off are E_{cut}=273 eV and E_{aug}=516 eV, respectively. For Si atoms, the valence system comprises the 3s and the 3p shell, and E_{cut} (E_{aug}) are set at 245 eV (322 eV).

In order to examine the reliability of the exchange-correlation functional on which the results of our manuscript are based, we carried out computations using the Perdew-Burke-Ernzerhoff (PBE) functional[44] for the cluster $CuSi_6$ as a test case. The optimizations performed with these two potentials yield the same type of equilibrium geometry, i.e. a substitutional structure based on the pentagonal shape of Si_7. The bond lengths obtained in the two cases deviate by about two per cent.

The atomic motion is described using Nosé dynamics[45] generating a canonical ensemble. The Nosé thermostat corresponds to a method for simulating a canonical ensemble at a selected temperature. The fictitious thermostat mass Q, which determines the response of the heat bath to fluctuations of the ionic system, must be sufficiently small to allow the system to approach equilibrium fast enough, and sufficiently large to yield correct values for the energy fluctuations of the ionic system.[46] In each individual case considered in the present work, we adjusted Q such that the period of the thermostat is equal to about 120 time steps.[35]

The ionic equations of motion are integrated using a fourth-order predictor-corrector algorithm[35,47,48] which allows the use of time steps as large as t=3.0 fs with good energy conservation.

In our simulation, the initial configuration was realized by a random distribution of atoms with 2.6 Å as the lower limit of the distance between any atom pair. Periodic boundary conditions were imposed on a cubic cell with of dimension 16 Å × 16 Å × 16 Å. By analyzing the atomic trajectories as they evolve during the simulation, we find that the minimal distance between atoms in neighboring supercells is larger than 9 Å, making the interaction between supercells negligible. Each simulation started at a temperature T=2000 K and was extended at this temperature over a period of 9.0ps (3000 time steps), allowing the system to attain equilibrium. Subsequently, the hot clusters were cooled down slowly and uniformly to zero temperature during a time interval of 30.0ps (10000 time steps). Finally, the geometry obtained from the simulated annealing procedure was optimized enforcing the convergence criterion that the difference between the total energies obtained in two subsequent steps be less than 0.1 meV. It should be noted that the value of the thermostat mass Q and the cooling speed are the most sensitive factors in the simulated annealing process. Performing several simulated annealing runs for selected test systems where the initial structure and the starting temperature were varied, we found the converged final structures unaffected by these procedural changes. In these tests, the starting temperature ranged from 2000 to 3000 K. However, variation of the value of Q and of the cooling speed resulted in alterations of the final structures. Especially, we observed that a combination of very small Q and fast cooling speed led, for some clusters, to isomers of higher energy. For standard simulated annealing runs, we implemented a cooling speed of 1^0 C/15 fs and a time step of 3 fs.

In order to confirm that the structure obtained by the process described above is the ground state, we also carried out geometry optimizations at the B3LYP/6−311+G(d,p) level for the lowest isomers that emerged from the simulated annealing procedure. A detailed discussion of the suitability of the B3LYP method for the treatment of metal – silicon clusters is presented in references [12] and [29]. The agreement of B3LYP results for various copper – silicon test cases with available experimental values and those obtained by quantum chemical procedures of higher accuracy was generally found to be very satisfactory. The quantum chemical calculations were performed using the Gaussian 03 code.[49] Three types of geometric arrangements were chosen as input structures, namely 1) geometries obtained from the above standard simulated annealing and the alternative process that combines a small value of Q with high cooling speed, leading to isomers of higher than the ground state energies, 2) substitutional structures of Si_7 (Cu_7,Li_7) with metallic atoms at the equatorial sites, 3) structures with face adsorption of the metallic atom on the Si_6^- framework for clusters of composition $MeSi_6$. Moreover, we subjected the isomers obtained using the B3LYP/6−311+G(d,p) approach to further optimization by means of the plane wave DFT method as implemented in the VASP program. The results are presented and discussed in the following section.

Results and discussion

The structures obtained from our simulated annealing approach and those generated by the quantum chemical computation are plotted in Figures 1 and 2. The isomers of the Cu_mSi_{7-m} series labeled as m**GS**, m**a,** m ≤ 6 are shown in Figure 1, where m**GS** refers to the geometry of the ground state (**GS**) obtained from simulated annealing, and m**a**, m**b**, ..., indicate the higher energy isomers obtained from the quantum chemical calculations with different initial structures as mentioned above. The results of Li_mSi_{7-m} are shown in Figure 2.

It is should be noted that the above **GS** of each cluster refers to the lowest energy state obtained from optimization by use of the plane wave (PW) DFT method. In each case, the **GS** is

employed as reference of zero energy. As can be seen from Table I, the results generated by use of the plane wave and the hybrid density functional (B3LYP) approaches are in a good agreement for all the isomers excepting the systems $CuSi_6$ and Cu_5Si_2. For all other isomers of the form Me_mSi_{7-m} (Me = Cu, Li), the difference between the geometric parameters obtained by use of the plane wave and the B3LYP method amounts to less than four per cent; thus in the following, the parameters referred to are those obtained by the latter procedure.

1. Cu_mSi_{7-m} (m=1,2,...,6)

We comment first on Cu_mSi_{7-m} ($m \leq 6$). Cu is one of the most widely used impurities in silicon device fabrication.[50] As shown by studies of transition metal elements in silicon, they tend to diffuse interstitially and locate at interstitial sites in thermal equilibrium at the diffusion temperature.[34] Investigations of copper doped silicon clusters demonstrate that Cu in Si_n is likely to occupy a substitutional position derived from the most stable geometry of Si_{n+1} by replacing a Si atom of obtained by Cu. The global minima of small Si_n clusters have been identified by extensive collaborative efforts of theory and spectroscopic measurement.[11]

The ground state of Si_7 (m=0) is a pentagonal bipyramid (D_{5h}).[10-12] The geometric parameters of Si_7 are much closer to anionic Si_6^- than to the neutral Si_6 cluster.[12] Two competitive geometries have been identified for the $CuSi_6$ (m=1) cluster. The lowest isomer (1**GS**) corresponds to a substitutional structure with Cu occupying an equatorial site. It is near-degenerate with an adsorption site isomer where Cu attaches to a face of the Si_6 frame. From DFT – plane wave calculation, these two alternatives are separated from each other by a small energy difference of 0.018 eV. It should be noted that the approach yields the same order of stabilities for the two structures[12]. The B3LYP/6−311+G(d,p) assessment favors the adsorption site (1**a**) over the substitutional site (1**GS**) by a still small but distinct energy difference of 0.078 eV. Both methods, however, predict the stabilities of the two compared structures to be almost equal.

For m=2, the equilibrium structure (2**GS**) involves two Cu atoms substituting for two Si atoms of the Si_7 cluster at equatorial sites. The 5 Si atoms arrange in a somewhat distorted D_{3h} structure, and the two Cu atoms form a dimer with an internuclear distance of 2.605Å. This value may be compared with the bond lengths of Cu_2 (2.278Å), and Cu_2^+ (2.449 Å). Thus, the bond distance of the Cu_2 subunit in Cu_2Si_5 is distinctly closer to that of the Cu_2 cation than that of the neutral molecule. This observation is in keeping with the result of natural population analysis[51], which implies that each Cu atom of Cu_2Si_5 transfers 0.45e to the Si subsystem, as indicated in Table II. On the other hand, an isomer with two Cu atoms replacing two Si atoms at the apical sites of Si_7 turns out to be higher in energy by 1.98 eV than 2**GS**, while that with two Cu atoms substituting for two equatorial Si atoms at separated sites is found to be unstable. The isomer of second to lowest stability (**2a**), being higher in energy than 2**GS** only by 0.070eV, is derived from the structure 1**a** of $CuSi_6$ with two Cu atoms at positions 1 and 3 (Figure 1). The architecture of this unit may be described as a Si_4 bent rhombus structure combined with two bonding Cu atoms and the remaining Si atom interacting with both the Si_4 and the Cu_2 subsystems.

The ground state of Cu_3Si_4 (3**GS**) is characterized by three Cu atoms substituting for three connected equatorial Si atoms. An initial substitutional structure with three disconnected Cu atoms at the equatorial sites of Si_7 relaxes to 3**a**, which is 0.073eV higher in energy than 3**GS**. As the 1**a** variant of $CuSi_6$ is prepared with three Cu atoms at positions 1, 3 and 7 (see Figure 1), relaxation to 3**a** is observed as well.

The ground state of Cu_4Si_3 (4**GS**) exhibits a deformed pentagonal shape, resembling the Si_7 species. The three Si atoms locate at the equatorial sites with two connected and one disconnected Si atoms. As demonstrated by natural population analysis[12], the apical Si atoms

of Si_7 accept electrons from the equatorial sites. This leads to the expectation that the two apical sites of the Cu_4Si_3 structure based on D_{5h} symmetry should be occupied by Si atoms. This structure, however, is shown to be unstable by B3LYP/6−311+(d,p) analysis. The Cu_4Si_3 ground state geometry may be understood as originating from the Cu_4 ground state which stabilizes as a bent rhombus. In Cu_4Si_3, the three Si atoms are adsorbed on different sides of this rhombus. An isomer (4**a**) with one Si atom adsorbed on the face of a Si_6-like Cu_4Si_2 framework is found to be 0.034eV higher in energy than 4**GS**. The isomer (4**b**) with one Si atom replacing Cu at an apical position and the other Si atoms occupying equatorial sites as defined by the Cu_7 matrix is 0.163 eV higher in energy than 4**GS**. It should be noted that the bent Cu_4 rhombus is present as a structural motif also in the isomer 4**a**.

Optimization employing the DFT - plane wave method shows that a structure derived from the D_{5h} prototype (5**GS**) defines the lowest energy state of Cu_5Si_2. DFT analysis at the B3LYP/6−311+G(d,p) level, in contrast, identifies a side adsorbed isomer (5**a**) with one Cu atom attached to a Si_6^--like framework consisting of the four remaining Cu atoms and two Si atoms as lower in energy than 5**GS** by 0.042eV. Both 5**GS** and 5**a** can be considered as one Cu atom adsorbed on a Si_6^--like substructure, where four Cu atoms form a bent Cu_4 rhombus, and two Si atoms locate above and below this rhombus. While simulated annealing at the standard settings employed in this work produces the 5**GS** unit, the alternative choice of parameters mentioned above, involving a small Nosé mass and fast cooling, yields 5**a**. The energy difference between these two alternatives is small, amounting to 0.078 eV as the DFT-plane wave method is used and to nearly one-half of this margin in case of the B3LYP treatment. A further isomer (5**b**) is found by DFT – plane wave calculation as 0.184eV higher in equilibrium energy than 5**GS**. In this case, four Cu atoms form a square, and two Si atoms adsorb on the top and bottom of it. A bipyramid structure (D_{4h}) results, to which the remaining Cu atom attaches by face adsorption.

The equilibrium structure of Cu_6Si (6**GS**) deviates from the D_{5h} scheme. Four Cu atoms form the corners of slightly distorted square. The Si atom is located above the center of this arrangement. Among the residual Cu atoms, one is adsorbed to a $SiCu_2$ face, and the other Cu atom bonds with a Cu_2 subgroup at the opposite side of the Cu_4 motif. This shape might be understood as resulting from the interaction between the pure D_{3h} Cu_6 cluster in its planar equilibrium geometry[22] with an adsorbed single Si atom. The isomer 6**a** is a structure with 5 Cu atoms and one Si atom forming a D_{4h} geometry with Si located at the top of the square defined by four Cu atoms. The remaining Cu occupies an adsorption site, interacting with a Cu_3 subgroup. Its energy is 0.217eV higher than that of 6**GS**. Both 6**GS** and 6**a** may be viewed as two Cu atoms adsorbed on a pyramid framework constructed by a Cu_4 square with Si top adsorption. The substitutional structure of Cu_7 with Si at an equatorial site (6**b**) is less stable than 6**GS** by 0.470eV, and that with Si at an apical site proves to be unstable.

Summarizing the observations made with respect to the preferred structures of the Cu_mSi_{7-m} series, we find a strong persistence of the pentagonal motif given by the equilibrium structures of the two homogeneous clusters Si_7 and Cu_7. This is plausible in the light of earlier work on $CuSi_n$ ($n \leq 6$)[12, 33] where it has been shown that Cu as an impurity in a Si_n cluster tends to occupy a substitutional site of Si_{n+1} and correspondingly interacts with its Si neighbors by forming covalent bonds with ionic admixtures. This statement, however, cannot be reversed, since, from the present work, the geometries of $CuSi_6$ and $SiCu_6$ turn out to differ substantially. This difference appears to be associated with the deviating equilibrium shapes of the pure clusters Si_6 and Cu_6, the former being three-dimensional and the latter planar. Our investigation suggests that m = 6 is the smallest number of Cu constituents in Cu_mSi_{7-m} for which the Cu_m subsystem exerts a defining influence on the geometry of the mixed cluster. The ground states of both Cu_4Si_3 and Cu_5Si_2, as well as their low-lying isomers, exhibit solvation of the 7-m Si atoms in the Cu_m subunit. These atoms do not form a connected subsystem, since at

least one of them bonds to Cu atoms only. The structure (3a) presents an example for the analogous phenomenon of Cu_m solvation in the Si_{7-m} subunit. This feature demonstrates a certain degree of miscibility of the two elements blended together in Cu_mSi_{7-m}.

2. Li_mSi_{7-m} (m=1,2,...,6)

The electronic structure of Lithium is $1s^22s^1$. The 2s electron transfers easily to silicon. From our calculations, we find that the ground states structures of Li_mSi_{7-m} tend to consist of an anionic Si_{7-m} framework surrounded by m Li atoms that act as electron donors. From natural population analysis, an electronic charge of about 0.8e transfers from each Li to Si atoms. In what follows, we comment on individual systems.

The ground state of $LiSi_6$ (1**GS**) is a deformed bipyramid, like the Si_7 matrix. The Li atom adsorbs on the Si_6^- framework at the equatorial site. The isomer (1**a**) with Li adsorbed on a Si_2 edge of Si_6^- framework is higher than 1**GS** by 0.264eV. The energy of isomer (1**b**), characterized by face adsorption of Li on Si_6^-, exceeds that of 1**GS** by 0.2734 eV, while a substitutional geometry based on Si_7 with Li located at the apical site is found to be less stable than 1**GS** by 2.009 eV. As a uniting structural feature of all explored $LiSi_6$ isomers (1**GS**, 1**a**, and 1**b**), the six Si atoms tend to arrange in a Si_6^- configuration, to which the Li atom is attached

The equilibrium structure (2**GS**) of Li_2Si_5 corresponds to adsorption of two Li atoms on two different faces of the trigonal bipyramid (D_{3h}) formed by five Si atoms. This Si_5 framework turns out to be more closely related to dianionic Si_5^{2-} than to neutral Si_5. To be specific, the 1Si-2Si and 2Si-4Si bond lengths and the 1Si-2Si-3Si angle of Li_2Si_5 are 2.483 Å, 2.411 Å and 105.580°, respectively, which are much closer to the corresponding parameters in Si_5^{2-} (2.400 Å, 2.606 Å, 102.391°) than in neutral Si_5 (2.329 Å, 3.124 Å, 78.489°). Other isomers (2**a** and 2**b**) represent face adsorption patterns involving two Li atoms on adjacent sides of Si_5^{2-}. Both are less stable than 2**GS**, by 0.016eV and 0.201eV, respectively. Isomer 2**a** is obtained by substituting two Li atoms for Si atoms at positions1 and 3 of 1**a** in $CuSi_6$. Isomer 2**b** arises from substituting two Li atoms for two equatorial atoms of Si_7. The salient feature of all of these isomers is that they derive from the Si_5^{2-} trigonal bipyramid, with both Li atoms selecting adsorption sites. Applying natural population analysis (Table II), we find an overall transfer of about 1.72e from the two Li atoms to Si_5. As a structural peculiarity of Si_5^{2-} in comparison with Si_5, the axis of the neutral species elongates markedly as two electrons are added to the cluster. A substitutional isomer (2**c**) based on Si_7, where two Li atoms occupy separated equatorial sites, is determined to be substantially higher in energy than 2**GS,** namely by 0.560eV.

As one goes to Li_3Si_4, a face adsorption geometry is identified for the ground state 3**GS**. The three Li atoms adsorb on three different sides of Si_4 which adopts tetrahedral geometry. This shape is incompatible with the Si_4 ground state which stabilizes as a planar rhombus (D_{2h}) in the neutral, cationic and anionic states.[12] The three-dimensional structure of Si_4^{2-}, however, is lower in energy by 0.188 eV than the planar rhombus alternative, as determined by optimization at the B3LYP/6−311+G(d,p) level. Natural population analysis shows that the three Li atoms transfer about 2.46e to Si_4. Thus, the case of Li_3Si_4 demonstrates once more that the Li components in the Si – Li composites considered here act as electron donors and further, that electron transfer proceeding from the metal subsystem sensitively determines the geometry adopted by the semiconductor subsystem. A further optimization was carried out on the basis of a substantially different initial geometry. More specifically, the $CuSi_6$ structure (1**a**) was used as a pattern, with Li atoms located at sites 1, 3, and 7 and Si atoms at the remaining sites. This configuration was found to relax to 3**GS**. The isomer (3**a**) obtained from an initial D_{5h} based structure where the three Li atoms are placed on connected equatorial positions is

0.374eV higher in energy than 3**GS**. The isomer (3**b**) involves adsorption of the three Li atoms on a bent Si_4 rhombus. This alternative, being less stable than 3**GS** by 0.493 eV, is not preferred.

The ground state geometry of Li_4Si_3 (4**GS**) differs strongly from that of Cu_4Si_3. The three Si atoms form an isosceles elongated Si_3 triangle; an Li_2 subunit bridges between the two Si atoms separated by the smallest distance within this Si_3 motif, and two Li atoms are symmetrically edge adsorbed at the two longer sides of Si_3. This isosceles elongated Si_3 triangle turns out to be more closely related to trianionic Si_3^{3-} than to neutral Si_3. To be specific, the 1Si-2Si (1Si-3Si) bond length in Li_4Si_3 is 2.363 Å, which is about 0.025 Å shorter than the corresponding parameter in Si_3^{3-}. Likewise, the distance between 2Si and 3Si of Li_4Si_3 is 2.715 Å, which is about 0.364 Å longer than the corresponding parameter in Si_3^{3-}. By comparing the relevant charge density distributions, we find the effective charges on the atoms 2Si and 3Si in Li_4Si_3 to be higher by 0.2e than those on their counterpart atoms in Si_3^{3-}. The interelectronic repulsion between 2Si and 3Si in Li_4Si_3 elongates the distance between them over that in Si_3^{3-}. The ground state has also been attained by employing an initial D_{5h} based structure with three Si atoms occupying one equatorial and two apical sites. No similarity is found between the geometry of the Li_4 subsystem of Li_4Si_3 and that of the free Li_4 cluster which has been shown to be planar[18, 20]. The isomer (4**a**) is obtained from an initial D_{5h} based structure with two Si atoms occupying connected equatorial sites and the other Si atom locating at a separate equatorial site, analogous to (1**a**) of $CuSi_6$ with three Si atoms occupying sites 4,5 and 6. This structure results as near degenerate with 4**GS,** as both geometries are separated by only 0.004eV. An isomer (4**b**) with one Li atom side-adsorbed on a Si_6–like framework formed by Li_3Si_3 exceeds 4**GS** by 0.341eV. This framework consists of two Li atoms adsorbed on the top and bottom of the Si_3 plane, and the additional Li atom on one of the longer sides of Si_3.

The equilibrium structure of Li_5Si_2 (5**GS**) possesses a high degree of symmetry. Four of the five Li atoms form a planar rhombus located below a Si dimer, above which the remaining Li atom adsorbs. A slightly different isomer (5**b**) with the four Li atoms arranged in a diamond structure is by 0.157eV higher than the 5**GS** energy. The isomer (5**a**) with four Li atoms assembled to form a square with one Si atom adsorbed above and the other below the plane defined by this substructure, and the residual Li atom face adsorbed is less stable by 0.149eV than 5**GS**.

Turning to Li_6Si (6**GS**), we find six octahedrally arranged Li atoms surrounding the central Si atom. The 6**GS** geometry is reproduced by B3LYP/6−311+G(d,p) optimization, where a D_{5h} based structure defines the initial geometry. The energy of a further isomer (6**a**) which derives from the $CuSi_6$ – (1**a**) prototype is 0.350 eV above that of 6**GS**.

On the basis of these observations, the members of the Li_mSi_{7-m} group stabilize in characteristically different equilibrium structures than their counterparts of the Cu_mSi_{7-m} series. While substitutional sites are selected by Cu as metal impurity, Li favors adsorption sites, related to different interaction modes of Cu and Li with the Si_{7-m} subsystem, namely the formation of covalent bonds in the former and stabilization through electron transfer in the latter case. This is in keeping with the observation that the natural charge on Li_m is substantially higher than that on Cu_m for all m considered. More specifically, Li_2Si_5 and Li_3Si_4 can be unambiguously described as Si_{7-m} dianions in contact with m Li adsorbate atoms, while Li_4Si_3 is more properly understood as involving a somewhat distorted Si_3^{3-} subunit. For m > 4, novel structures are found as the resulting Li_mSi_{7-m} equilibrium geometries appear to be dictated neither by the Li_m nor by the Si_{7-m} subsystem.

3. Energy gaps

It is interesting to examine if the expected narrowing trend of the energy gap as one goes from the purely semiconducting Si_7 system to the purely metallic clusters Li_7 and Cu_7 can be confirmed for the systems investigated in this work. The results emerging from our plane wave basis and B3LYP/6−311+G(d,p) calculations are listed in Table I. Only the closed-shell clusters are included, i.e., Me_mSi_{7-m} with m=0, 2, 4, 6. Consistently, the energy gaps obtained by the DFT plane-wave method are smaller than those determined by use of the hybrid quantum chemical technique by about 1.1 eV. The energy gap 2.097 eV of Si_7 is the same as indicated in reference [7]. A slight reduction of the energy gaps is observed as two metal atoms replace two Si atoms. This moderate change is followed by a drastic decrease as the metal atom count is incremented from two to four. As we proceed to larger complexes, however, the energy gap is found to increase from 1.002eV in Cu_4Si_3 to 1.725eV in Cu_6Si. It is worth while noting that this conspicuous deviation from the trend suggested by the complexes with fewer Cu atoms correlates with geometry. Thus, the ground state structure of Cu_6Si differs strongly from those of Si_7, Cu_2Si_5, and Cu_4Si_3 which are all variations of the pentagonal pattern defined by the 'limiting clusters' Si_7 and Cu_7. The corresponding Cu_6Si isomer (6**b**) exhibits an energy gap of 0.409eV which is drastically reduced as compared to that of Cu_4Si_3, namely by about 0.6eV. Therefore, by the criterion of energy gap size, the sequence of Cu_mSi_{7-m} isomers with D_{5h} based geometries displays the anticipated trend of increasing metallicity with the number m of metal atoms contained in the cluster. Within the series of the maximally stable Cu_mSi_{7-m} systems, the unit Cu_6Si presents an exception from this rule.

A similar, although more homogeneous picture is presented by the Li_mSi_{7-m} series where an energy gap reduction from m = 0 to m = 4 is contrasted by a slight increase as one goes from m = 4 to m = 6. This observation is based on the DFT plane wave results, while the B3LYP/6−311+G(d,p) data predict a consistently decreasing trend. In spite of the obvious preponderance of the metal atom component in Li_6Si and its peculiar geometry, involving a Si atom octahedrally surrounded by a metal atom shell, both the geometric parameters and the natural charges on the atomic centers of this cluster suggest that it cannot be characterized as metallic. The distance between adjacent Li atoms of d(Li – Li) = 3.4 Å, which is markedly elongated by the standard of bond lengths found typically in small Li_m clusters ($m \leq 6$) [18], diminishes the interaction between these ligands. Instead, the natural charges listed in Table 2 document a substantial amount of electron transfer from each metal atom to the Si center, giving rise to a complex of pronounced polarity. In view of these features, an energy gap narrowing as one goes from Li_4Si_3 to Li_6Si is not a cogent conclusion.

Summary

The ground state geometries and associated energetic properties of the cluster series Me_mSi_{7-m} (Me=Cu and Li, $m \leq 6$) were identified by simulated annealing computations, the use of a global search algorithm being necessitated by the large number of possible atomic permutations for Me_mSi_{7-m} with $1<m<6$. Equilibrium geometries are obtained by use of a DFT - plane wave formalism in conjunction with the Nosé thermostat scheme. Good agreement is found between the DFT - plane wave basis method and the hybrid quantum chemical method B3LYP at the 6−311+G(d,p) level, excepting the cases of $CuSi_6$ and Cu_5Si_2 where the D_{5h} based shapes yielded by the former approach deviate from the geometries resulting from the latter. Within an accuracy of 0.1 eV, however, the order of stabilities among the ground state systems and low-lying isomers as predicted by the two methods agree in all cases considered.

Focusing on the general trends of the ground state equilibrium geometries of Me_mSi_{7-m} (Me = Li and Cu, $m \leq 6$), one observes that Cu_mSi_{7-m} tends to stabilize in D_{5h} based substitutional geometries, while Li_mSi_{7-m} prefers adsorption geometries, involving m Li atoms attached to a Si_{7-m}^{2-} (or Si_{7-m}^{3-}) framework whose architecture is determining for the shape of the cluster

as a whole. For Cu_mSi_{7-m}, an exception from the prevailing pentagonal pattern is given by the system Cu_6Si where the Si atom is adsorbed to a deformed Cu_6 substructure. In contrast, none of the Li_m subsystems resulting from Li_mSi_{7-m} optimization bear resemblance to the geometries of any free Li_m clusters. The observed preference of the pentagonal prototype as the structure of Cu_mSi_{7-m} clusters suggests a certain extent of interchangeability of Cu and Si constituents in these systems. This trend is further substantiated by the ground state configurations of the species with m = 2, 3 where fragmentation of the Si_{7-m} is obtained.

The energy gaps of Me_mSi_{7-m} (Me = Cu and Li, $m \leq 6$) display a narrowing trend with the number of metal constituents, reflecting the increase of cluster metallicity. The species with m = 6, however, do not conform with this general tendency. This exceptional behavior appears correlated with the geometric characteristics of the two systems. While Cu_6Si drastically deviates from the D_{5h} based motif that dominates the Cu_mSi_{7-m} series, Li_6Si displays octahedral coordination, giving rise to substantial polarity between the Si core and the Li_6 ligand shell.

It will be interesting to extend the present study into the region of mixed metal – semiconductor clusters of intermediate size, with $10 \leq m \leq 50$. Besides its fundamental relevance for the understanding of atomic clusters, such an investigation could contribute to answering the topical question to what degree various metal elements can be solvated in finite semiconductor structures.

Acknowledgments

This work is supported by the National Science Foundation through the grants HRD-9805465, NSFESP-0132618 and DMR-0304036, by the National Institute of Health through the grant S06-GM008047, and by the Army High Performance Computing Research Center under the auspices of Department of the Army, Army Research Laboratory under Cooperative Agreement No. DAAD 19-01-2-0014.

References

1. Baletto F, Ferrando R. Rev. Mod. Phys 2005;77:1.
2. Henry CR. Surf. Sci. Rep 1998;31:235.
3. Alivisatos AP. Sci. Am. Int. (Ed.) 2001;285:66.
4. Alivisatos AP, Johnsson KP, Peng XG, Wilson TE, Loweth CJ, Bruchez MP, Schultz PG. Nature (London) 1996;382:609. [PubMed: 8757130]
5. Bloomfield LA, Freeman RR, Brown WL. Phys. Rev. Lett 1985;54:2246. [PubMed: 10031290]
6. Martin TP, Schaber H. J. Chem. Phys 1985;83:855.
7. Lu ZY, Wang CZ, Ho KM. Phys. Rev. B 2000;61:2329.
8. Rata I, Shvartsburg AA, Horoi M, Frauenheim Th. Siu KWM, Jackson KA. Phys. Rev. Lett 2000;85:546. [PubMed: 10991336]
9. Sieck A, Porezag D, Frauenheim Th. Peterson MR, Jackson KA. Phys. Rev. A 1997;56:4890.
10. Raghavachari K, Rohlfing CM. J. Chem. Phys 1991;94:3670.Raghavachari K, Rohlfing CM. J. Chem. Phys 1988;89:2219.
11. Shvartsburg AA, Liu B, Jarrold MF, Ho KM. J. Chem. Phys 2000;112:4517.
12. Xiao C, Hagelberg F, Lester WA Jr. Phys. Rev. B 2002;66:075425.
13. Jackson KA, Horoi M, Chaudhuri I, Frauenheim Th, Shvartsburg AA. Phys. Rev. Lett 2004;93:013401.
14. Prendergast D, Grossman JC, Williamson AJ, Fattebert J–L, Galli G. J. Am. Chem. Soc 2004;126:13827. [PubMed: 15493943]
15. Marim LR, Lemes MR, Dal Pino A Jr. Phys. Rev. A 2003;67:033203.
16. Knight WD, Clemenger K, de Heer WA, Saunders WA, Chou MY, Cohen ML. Phys. Rev. Lett 1984;52:2141.
17. Bonacic-Koutecký V, Fantucci P, Koutecký J. Phys. Rev. B 1988;37:4369.

18. Boustani I, Pewestorf W, Fantucci P, Bonacic-Koutecký V, Koutecký J. Phys. Rev. B 1987;35:9437.
19. Ishikawa Y, Sugita Y, Nishikawa T, Okamoto Y. Phys. Lett. A 2001;333:199.
20. Srinivas S, Jellinek J. Phys. Status Solidi 2000;217:311.
21. Alonso JA. Chem. Rev. (Washington, D.C.) 2000;100:637.
22. Jug K, Zimmermann B, Calaminici P, Köster AM. J. Chem. Phys 2002;116:4497.
23. Fujima N, Yamaguchi T. J. Phys. Soc. Jpn 1989;58:1334.
24. Beck SM. J. Chem. Phys 1989;90:6306.
25. Hiura H, Miyazaki T, Kanayama T. Phys. Rev. Lett 2001;86:1733. [PubMed: 11290235]
26. Han JG, Shi YY. Chem. Phys 2001;266:33.
27. Han JG, Hagelberg F. Chem. Phys 2001;263:55.
28. Xiao C, Hagelberg F. J. Mol. Structure: THEOCHEM 2000;529:241.
29. Ovcharenko IV, Lester WA Jr. Xiao C, Hagelberg F. J. Chem. Phys 2001;114:9028.
30. Kumar V, Kawazoe Y. Phys. Rev. Lett 2001;87:045503. [PubMed: 11461629]
31. Scherer JJ, Pau JB, Collier CP, Saykally RJ. J. Chem. Phys 1995;102:5190.ibid. 103, 113 (1995)
32. Scherer JJ, Pau JB, Collier CP, O'Keefe A, Saykally RJ. J. Chem. Phys 1995;103:9187.
33. Xiao C, Abraham A, Quinn Q, Hagelberg F, Lester WA Jr. J. Phys. Chem 2002;106:11380.
34. Weber ER. Appl. Phys. A: Mater. Sci. & Proc 1983;30:1.
35. Kresse G, Hafner J. Phys. Rev. B 1993;47:558.Kresse G, Hafner J. Phys. Rev. B 1994;49:14251.
36. Kresse G, urthmuller JF. Comput. Mater. Sci 1996;6:15.
37. Mermin ND. Phys. Rev 1965;140:A1141.
38. Perdew JP, Zunger A. Phys. Rev. B 1981;23:5048.
39. Kohn W, Sham LJ. Phys. Rev 1965;140:A1133.
40. Wood DM, Zunger A. J. Phys. A 1985;18:1343.
41. Pulay P. Phys. Lett 1980;73:393.
42. Blöchl PE. Phys. Rev. B 1994;50:17953.
43. Perdew JP, Wang Y. Phys. Rev. B 1992;45:13244.
44. Perdew JP, Burke K, Ernzerhof M. Phys. Rev. Lett 1996;77:3865. [PubMed: 10062328]
45. Nosé S. J. Chem. Phys 1984;81:511.
46. Bylander DM, Kleinman L. Phys. Rev. B 1992;46:13756.
47. Gear, CW. Numerical Initial Value Problem in Ordinary Differential Equations. Prentice Hall, Englewood Cliffs; NJ: 1971. Chap. 9 and 10
48. Arnold A, Mauser N, Hafner J. J. Phys. Condens. Matter 1989;1:965.
49. Frisch, MJ.; Trucks, GW.; Schlegel, HB.; Scuseria, GE.; Robb, MA.; Cheeseman, JR.; Montgomery, JA., Jr.; Vreven, T.; Kudin, KN.; Burant, JC.; Millam, JM.; Iyengar, SS.; Tomasi, J.; Barone, V.; Mennucci, B.; Cossi, M.; Scalmani, G.; Rega, N.; Petersson, GA.; Nakatsuji, H.; Hada, M.; Ehara, M.; Toyota, K.; Fukuda, R.; Hasegawa, J.; Ishida, M.; Nakajima, T.; Honda, Y.; Kitao, O.; Nakai, H.; Klene, M.; Li, X.; Knox, JE.; Hratchian, HP.; Cross, JB.; Bakken, V.; Adamo, C.; Jaramillo, J.; Gomperts, R.; Stratmann, RE.; Yazyev, O.; Austin, AJ.; Cammi, R.; Pomelli, C.; Ochterski, JW.; Ayala, PY.; Morokuma, K.; Voth, GA.; Salvador, P.; Dannenberg, JJ.; Zakrzewski, VG.; Dapprich, S.; Daniels, AD.; Strain, MC.; Farkas, O.; Malick, DK.; Rabuck, AD.; Raghavachari, K.; Foresman, JB.; Ortiz, JV.; Cui, Q.; Baboul, AG.; Clifford, S.; Cioslowski, J.; Stefanov, BB.; Liu, G.; Liashenko, A.; Piskorz, P.; Komaromi, I.; Martin, RL.; Fox, DJ.; Keith, T.; Al-Laham, MA.; Peng, CY.; Nanayakkara, A.; Challacombe, M.; Gill, PMW.; Johnson, B.; Chen, W.; Wong, MW.; Gonzalez, C.; Pople, JA. Gaussian 03, Revision C.02. Gaussian, Inc.; Wallingford CT: 2004.
50. Istratov AA, Weber ER. Appl. Phys. A 1998;66:123.
51. Foster JP, Weinhold F. J. Am. Chem. Soc 1980;102:7211.Reed AE, Weinhold F. J. Chem. Phys 1983;78:4066.Reed AE, Weinstock RB, Weinhold F. J. Chem. Phys 1985;83:735.

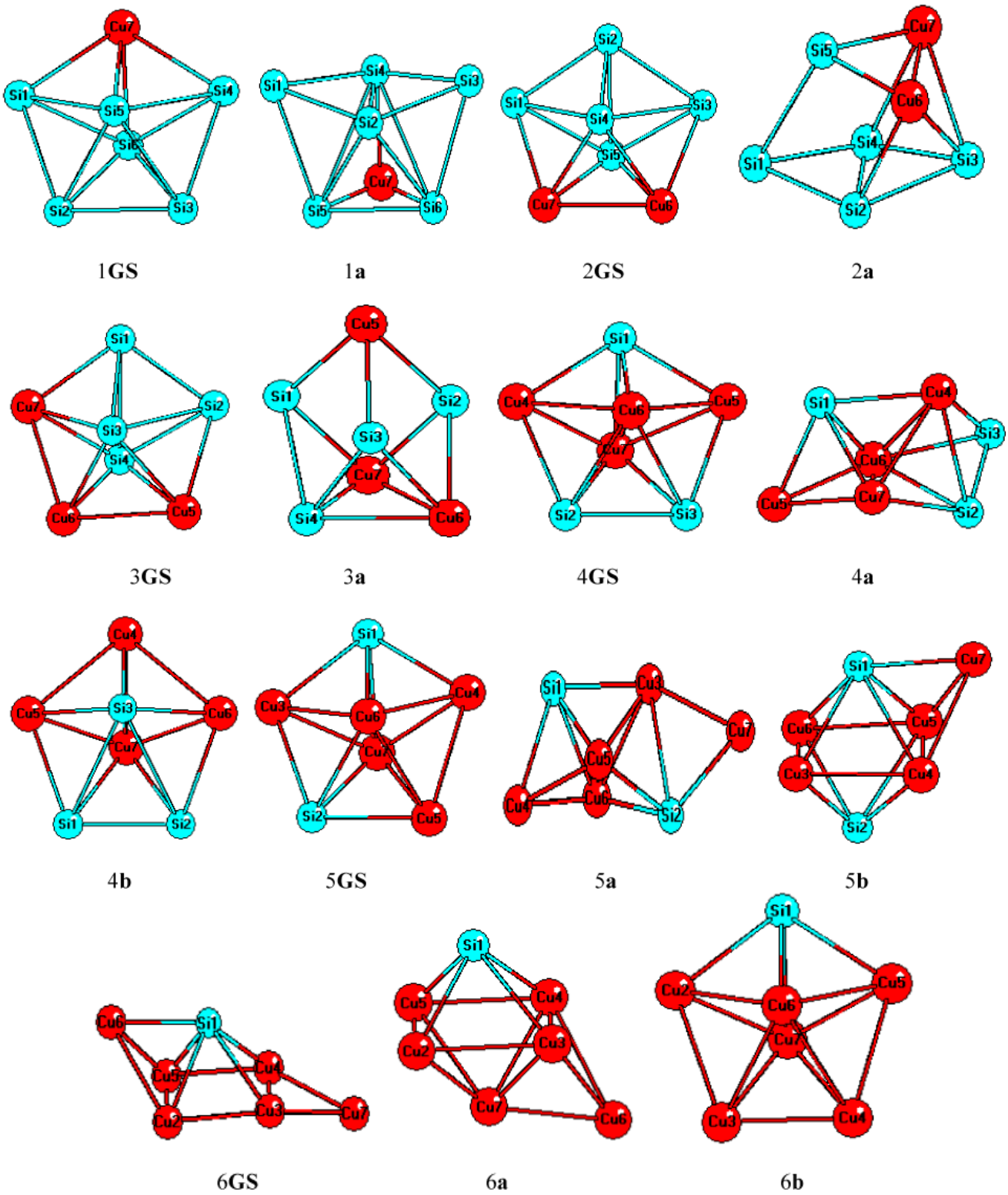

Figure 1.
The structure of Cu_mSi_{7-m} (m=1,2,...,6) clusters

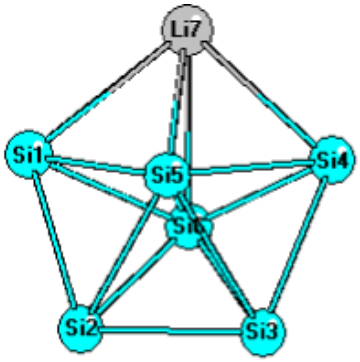

1GS

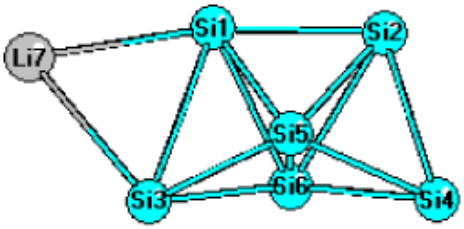

1a

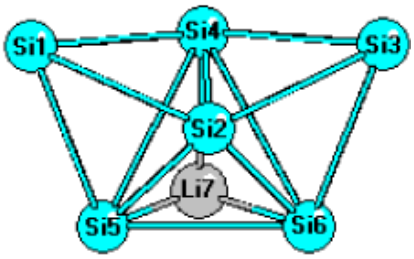

1b

2GS

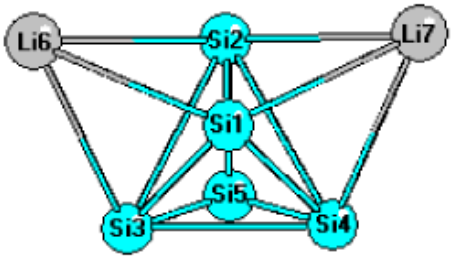

2a

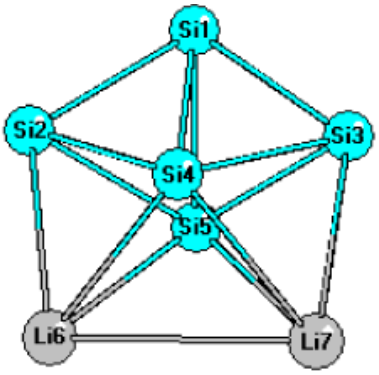

2b

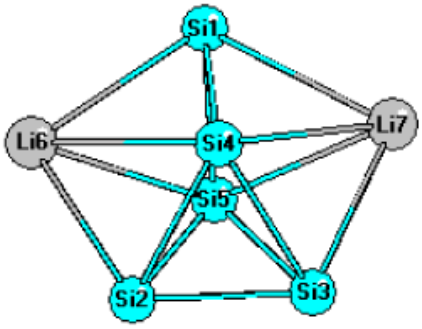

2c

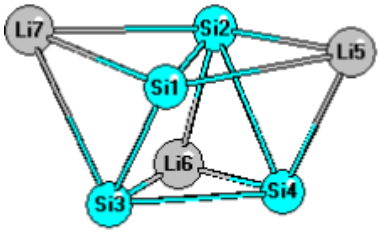

3GS

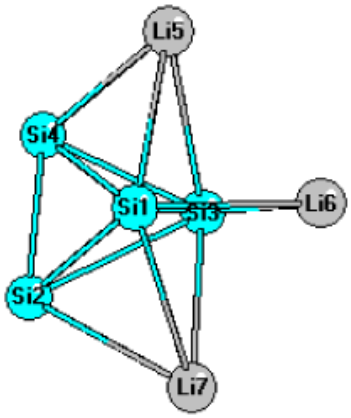

3a

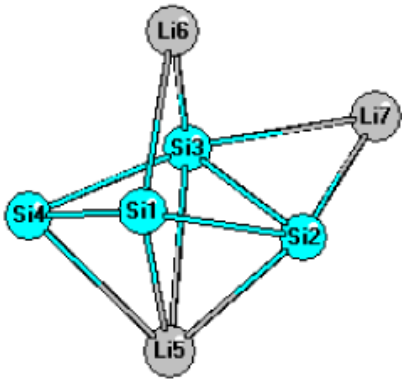

3b

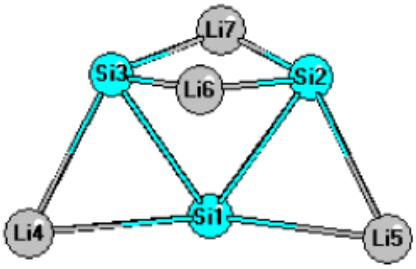

4GS

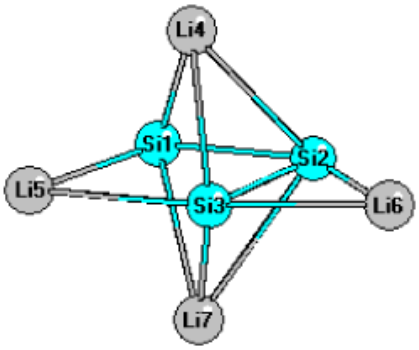

4a

4b

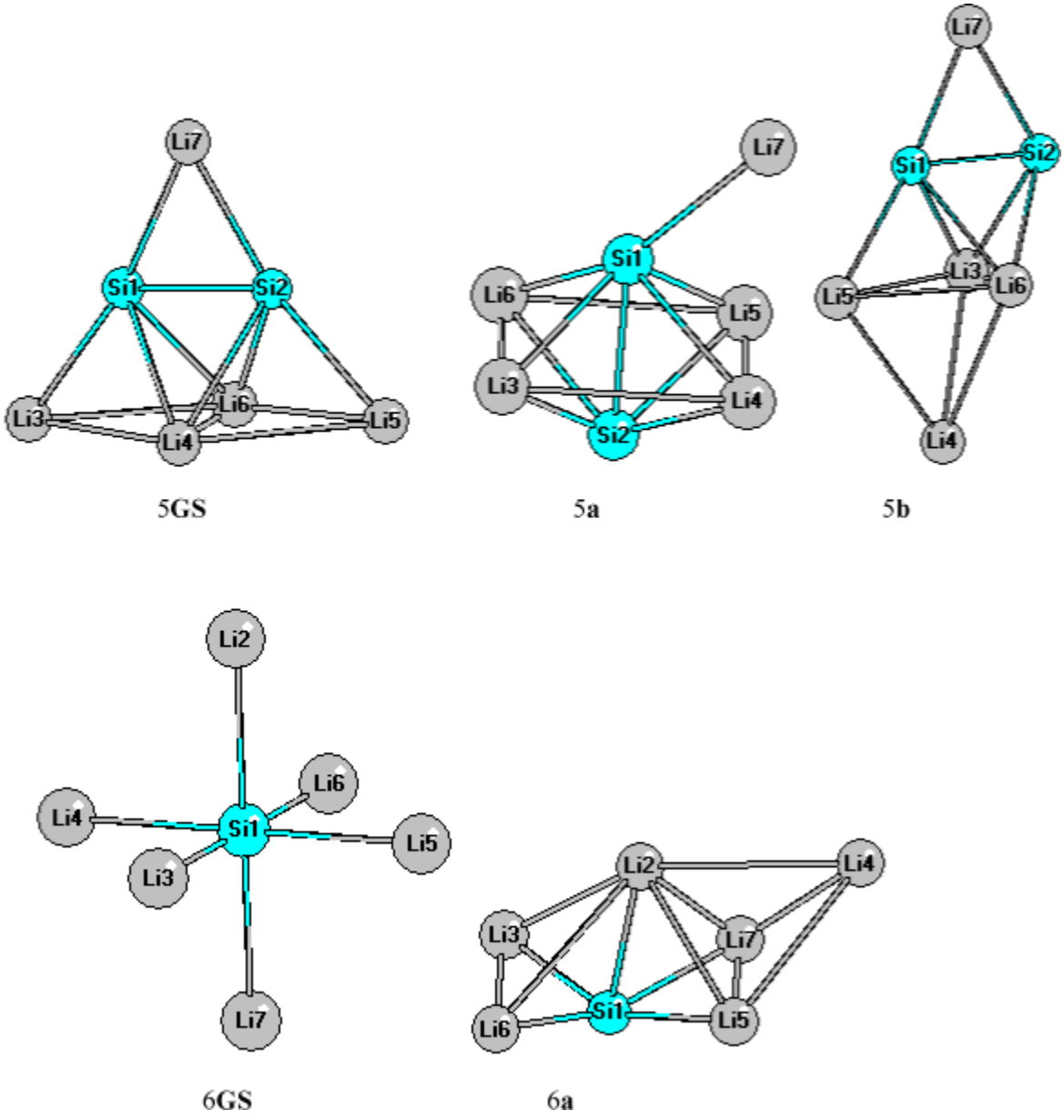

Figure 2.
The structure of Li_mSi_{7-m} (m=1,2,...,6) clusters

Table I

Relative energies and energy gaps for considered clusters with different isomers

Cluster	Isomer	Relative energy(eV)		Energy gap(eV)	
		PW DFT	B3LYP	PW DFT	B3LYP
Si_7	0**GS**	0.0	0.0	2.097	3.162
$CuSi_6$	1**GS**	0.0	0.00		
	1**a**	0.018	−0.078		
Cu_2Si_5	2**GS**	0.0	0.0	1.827	3.054
	2**a**	0.070	0.072		
Cu_3Si_4	3**GS**	0.0	0.0		
	3**a**	0.073	0.120		
Cu_4Si_3	4**GS**	0.0	0.0	1.002	2.179
	4**a**	0.034	0.005		
	4**b**	0.163	0.104		
Cu_5Si_2	5**GS**	0.00	0.0		
	5**a**	0.071	−0.042		
	5**b**	0.184	0.140		
Cu_6Si	6**GS**	0.0	0.0	1.725	2.602
	6**a**	0.217	0.242	0.893	1.890
	6**b**	0.470	0.627	0.409	1.450
$LiSi_6$	1**GS**	0.0	0		
	1**a**	0.264	0.199		
	1**b**	0.273	0.254		
Li_2Si_5	2**GS**	0	0	2.103	3.188
	2**a**	0.016	0.025		
	2**b**	0.201	0.230		
	2**c**	0.560	0.494		
Li_3Si_4	3**GS**	0	0		
	3**a**	0.374	0.365		
	3**b**	0.493	0.380		
Li_4Si_3	4**GS**	0	0	0.915	1.910
	4**a**	0.004	0.008		
	4**b**	0.341	0.311		
Li_5Si_2	5**GS**	0	0		
	5**a**	0.149	0.107		
	5**b**	0.157	0.092		
	5**c**	0.283	0.250		
Li_6Si	6**GS**	0	0	1.025	1.530
	6**a**	0.350	0.357	0.944	1.679

Table II

Natural charge for all atoms in selected isomers by Gaussian at B3LYP/6−311+G(d,p). The red color refers to Cu, the grey color to Li atoms.

Cluster	Isomer	1	2	3	4	5	6	7
$CuSi_6$	1**a**	0.12	−0.25	0.12	−0.31	−0.10	−0.10	0.52
Cu_2Si_5	2**GS**	−0.03	−0.23	−0.03	−0.29	−0.32	0.45	0.45
Cu_3Si_4	3**GS**	−0.24	−0.24	−0.40	−0.40	0.45	0.39	0.45
Cu_4Si_3	4**GS**	−1.02	−0.44	−0.44	0.47	0.47	0.48	0.48
Cu_5Si_2	5**a**	−0.84	−0.83	0.38	0.30	0.37	0.37	0.25
Cu_6Si	6**GS**	−1.25	0.27	0.34	0.34	0.27	0.27	−0.24
$LiSi_6$	1**GS**	−0.10	0.05	0.06	−0.10	−0.38	−0.38	0.85
Li_2Si_5	2**GS**	−0.15	−0.37	−0.15	−0.68	−0.37	0.86	0.86
Li_3Si_4	3**GS**	−0.53	−0.84	−0.56	−0.53	0.84	0.81	0.81
Li_4Si_3	4**GS**	−0.83	−1.27	−1.27	0.85	0.85	0.83	0.85
Li_5Si_2	5**GS**	−1.47	−1.47	0.55	0.49	0.55	0.49	0.88
Li_6Si	6**GS**	−3.60	0.60	0.60	0.60	0.60	0.60	0.60

J Phys Chem A. Author manuscript; available in PMC 2008 December 1.